



# Synthesis and Characterization of Covalent Triazine Framework CTF-1@Polysulfone Mixed Matrix Membranes and Their Gas Separation Studies

Subarna Dey<sup>1†</sup>, Stefanie Bügel<sup>1†</sup>, Sara Sorribas<sup>2</sup>, Alexander Nuhnen<sup>1</sup>, Asamanjoy Bhunia<sup>1</sup>, Joaquín Coronas<sup>2</sup> and Christoph Janiak<sup>1\*</sup>

<sup>1</sup> Institut für Anorganische Chemie und Strukturchemie, Heinrich-Heine-Universität Düsseldorf, Düsseldorf, Germany,

<sup>2</sup> Chemical and Environmental Engineering Department and Instituto de Nanociencia de Aragón, Instituto de Ciencia de Materiales de Aragón (ICMA), Universidad de Zaragoza-CSIC, Zaragoza, Spain

## OPEN ACCESS

### Edited by:

Xuezhong He,  
Norwegian University of Science and  
Technology, Norway

### Reviewed by:

Evangelos Favvas,  
Institute of Nanoscience and  
Nanotechnology, National Centre of  
Scientific Research  
Demokritos, Greece  
Xiangshu Chen,  
Jiangxi Normal University, China

### \*Correspondence:

Christoph Janiak  
janiak@uni-duesseldorf.de

<sup>†</sup>These authors have contributed  
equally to this work

### Specialty section:

This article was submitted to  
Chemical and Process Engineering,  
a section of the journal  
Frontiers in Chemistry

**Received:** 09 August 2019

**Accepted:** 07 October 2019

**Published:** 23 October 2019

### Citation:

Dey S, Bügel S, Sorribas S, Nuhnen A,  
Bhunia A, Coronas J and Janiak C  
(2019) Synthesis and Characterization  
of Covalent Triazine Framework  
CTF-1@Polysulfone Mixed Matrix  
Membranes and Their Gas Separation  
Studies. *Front. Chem.* 7:693.  
doi: 10.3389/fchem.2019.00693

Covalent triazine framework CTF-1 and polysulfone (PSF) are used to form mixed-matrix membranes (MMMs) with 8, 16, and 24 wt% of the porous filler material CTF-1. Studies on permeability and selectivity are carried out concerning the gases O<sub>2</sub>, N<sub>2</sub>, CO<sub>2</sub>, and CH<sub>4</sub>. CO<sub>2</sub> permeability of the synthesized MMMs increases by 5.4 Barrer in comparison to the pure PSF membrane. The selectivity remains unchanged for O<sub>2</sub>/N<sub>2</sub> and CO<sub>2</sub>/CH<sub>4</sub> but was found to be increased for CO<sub>2</sub>/N<sub>2</sub>. Further, comparisons to theoretical models for permeability prediction yield a permeability for CTF-1 which is about six times higher than the permeability of PSF. The inverse of the sum of the free fractional volumes (FFV) of the polymer and the filler correlate linearly to the logarithm of the permeabilities of the gases which conversely indicates that the porosity of the filler contributes to the gas transport through the membrane.

**Keywords:** covalent triazine framework (CTF), polysulfone (PSF), mixed-matrix membrane (MMM), gas selectivity, free fractional volume

## INTRODUCTION

During the last decades membrane-based separation technology has experienced a major expansion in the gas separation industry due to advantages like low operating costs, ease of operation, minimum energy requirement, and environmental friendliness. Currently membrane-based technology is used in the chemical and petrochemical industry, for natural gas purification, hydrogen separation, nitrogen recovery, and olefin/paraffin separation (Koros and Fleming, 1993; Strathmann, 2001; Baker, 2002; Zhang et al., 2008). Polymeric membranes have been studied widely for their low costs, high processability, and good intrinsic transport properties. However, pure polymer membranes face a reciprocal trade-off relationship between permeability and selectivity (Shimekit et al., 2011). Inorganic membranes, in spite of having outstanding separation properties, good thermal, mechanical and chemical stability, suffer from high production costs, lack of processability, difficulties in large-scale production, and brittleness (Dong et al., 2013). As an alternative to polymer and inorganic membranes, mixed matrix membranes (MMMs) have attracted major attention due to their low costs, high permeabilities, and possibly selectivities above the Robeson upper-bound limit (Dong et al., 2013). A typical MMM contains a bulk

continuous polymer phase and a dispersed inorganic particle phase. Polymers that are generally used to fabricate MMMs include polysulfone, polyarylates, polycarbonates, poly(arylethers), poly(arylketones), and polyimides (Tanh Jeazet et al., 2012). Porous materials that are generally incorporated to fabricate MMMs are carbon molecular sieves, zeolites, mesoporous materials, activated carbons, carbon nanotubes, and metal organic frameworks (MOFs) (Buonomenna et al., 2012; Tanh Jeazet et al., 2012; Bastani et al., 2013; Dong et al., 2013). In recent years porous organic polymers (POPs) or covalent organic frameworks (COFs) have also been explored to fabricate such membranes (Dechnik et al., 2017).

A subcategory of POPs/COFs are nitrogen-rich covalent triazine frameworks (CTFs). CTFs were first developed by Kuhn et al. by a polymerization reaction of aromatic di- or trinitrile building blocks under ionothermal conditions at 400–700°C using an excess of ZnCl<sub>2</sub>. The latter acts as a Lewis acid catalyst and solvent (porogen) for the polymerization reaction (Kuhn et al., 2008). Up to now, only few examples of CTF membranes were reported. Tang et al. reported an *in situ* fabricated neat CTF-membrane made from 4,4'-biphenyldicarbonitrile, which exhibits a high water permeability of 75600 Barrer and a water/ethanol selectivity of 101 for the dehydration of an 85 wt% ethanol aqueous solution at 45°C (Tang et al., 2015). Ying et al. developed a strategy for a graphene-oxide assisted restacking method to fabricate an ultrathin CTF-1 membrane, which showed a H<sub>2</sub>/CO<sub>2</sub> selectivity of 22.3 (Ying et al., 2016).

High surface area, low density, excellent thermal and chemical stability with a large number of nitrogen functionalities make CTFs potential candidates for gas storage and separation (Bhunia et al., 2013; Dey et al., 2017). These facts suggested us to fabricate MMMs by using CTF-1 as a filler. The glassy polymer PSF was chosen as a matrix due to its good mechanical properties including a good film-formation behavior (Dechnik et al., 2016). The prepared MMMs (8, 16, and 24 wt% of CTF-1) were tested for O<sub>2</sub>/N<sub>2</sub>, CO<sub>2</sub>/N<sub>2</sub>, and CO<sub>2</sub>/CH<sub>4</sub> separation.

## MATERIALS AND METHODS

### Materials

All chemicals were purchased from commercial suppliers (Sigma-Aldrich, Acros Organics, and Alfa Aesar chemical company). Polysulfone (PSF) Ultrason S 6010 Natural was provided by BASF AG, Ludwigshafen, Germany. The gases O<sub>2</sub>, N<sub>2</sub>, CO<sub>2</sub>, and CH<sub>4</sub> were supplied by Air Liquide (Germany) and used as received (purity 99.99%).

### Methods

Elemental analysis (CHN) was carried out on a PerkinElmer 2400 series 2 elemental analyzer. Thermal gravimetric analysis (TGA) was performed on a Netzsch TG 209 F3 Tarsus thermal gravimetric analyzer with a ramp rate of 5°C/min. A Bruker FT-IR Tensor 37 Spectrometer was used to obtain infrared (IR) spectra in the 4,000–550 cm<sup>-1</sup> region with a 2 cm<sup>-1</sup> resolution. Measurements were carried out on KBr disks. Powder X-ray diffraction (PXRD) was performed on a Bruker D2 Phaser diffractometer using Cu K<sub>α1/α2</sub> radiation with λ = 1.5418 Å

at 30 kV. 2θ angles in the range of 5–80° over a time of 2 h (0.01°/sec) were covered. Scanning electron microscopy (SEM) images were created by using a secondary electron (SE) detector equipped ESEM Quanta 400 FEG SEM. Sorption isotherms were obtained from a Micromeritics ASAP 2020 automatic gas sorption analyzer equipped with an oil-free vacuum pump (ultimate vacuum <10<sup>-8</sup> mbar). Selectivity factors based on ideal adsorbed solution theory (IAST) were calculated using the software 3Psim version 1.1.0.7. Skeletal density was determined with a Helium pycnometer, Micromeritics AccuPyc 1330.

For determination of the permeability of the membranes, firstly the thickness of the membranes was measured on 10 different points using a micrometer screw. The gas permeation experiments were performed as described by Tanh Jeazet et al. (2016). The membrane with an area of 11.3 cm<sup>2</sup> was placed into a permeation cell. First the permeate side was evacuated followed by evacuation of the feed side. The valve on the feed side was kept closed while pressurizing to approximately 3 bar for 2 h with a single gas. The line between vacuum pump and permeate side was closed followed by the adjustment of the feed pressure. The pressure on the permeate side was increased as the gas permeated from the feed side through the membrane to the permeate side. The linear rise of the pressure, recorded with an x-y printer, was used to calculate the permeability *P* in Barrer units.

Permeability is defined as the gas flow rate multiplied by the thickness of the material, divided by the area and by the pressure difference across the material:

$$\text{Permeability } (P) = \frac{\text{flow rate} \times \text{thickness}}{\text{area} \times \text{pressure difference}} \quad (1)$$

$$P(1\text{Barrer}) = 10^{-10} \times \frac{\text{cm}^3(\text{STP}) \times \text{cm}}{\text{cm}^2 \times \text{s} \times \text{cmHg}} \quad (2)$$

In the CGS system permeability can also be expressed as follows:

$$P = \frac{g \times \text{cm}}{\text{sec} \times \text{cm}^2 \times (\text{dyne} \times \text{cm}^{-2})} \quad (3)$$

The relationship between the different units is given as:

$$1 \left[ \frac{g \times \text{cm}}{\text{sec} \times \text{cm}^2 \times (\text{dyne} \times \text{cm}^{-2})} \right] = \frac{(2.9882 \times 10^{18})}{M} \left[ 10^{-10} \times \frac{\text{cm}^3(\text{STP}) \times \text{cm}}{\text{sec} \times \text{cm}^2 \times \text{cmHg}} \right] \quad (4)$$

The ideal gas selectivity was calculated from the single gas permeabilities by using the following equation:

$$\alpha_{\text{ideal}} \left( \frac{\text{O}_2}{\text{N}_2} \right) = \frac{P_{\text{O}_2}}{P_{\text{N}_2}} \quad (5)$$

### Synthesis of CTF-1

CTF-1 has been synthesized according to the following procedure (Kuhn et al., 2008): a mixture of terephthalonitrile (1.28 g, 10 mmol) and anhydrous ZnCl<sub>2</sub> (6.8 g, 50 mmol) was placed into a Pyrex ampoule under inert conditions. The ampoule was evacuated, sealed, and heated for 48 h at 400°C followed by

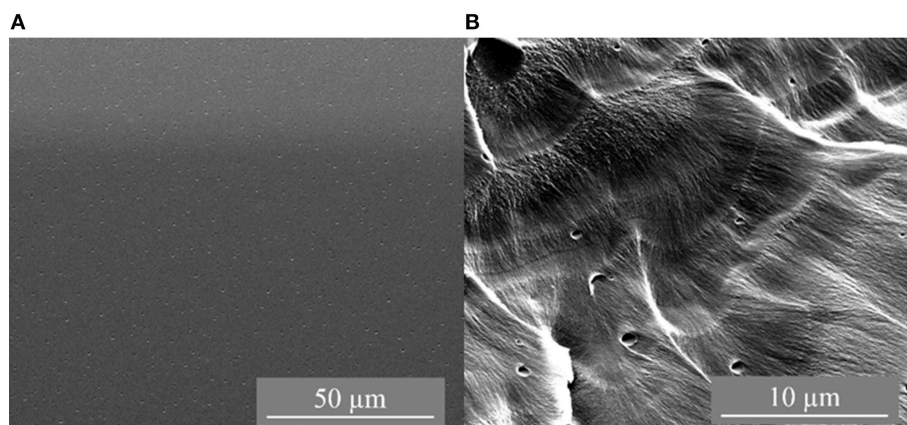


**FIGURE 1** | SEM images of pure PSF membrane [(A): top side view; (B): cross section view].

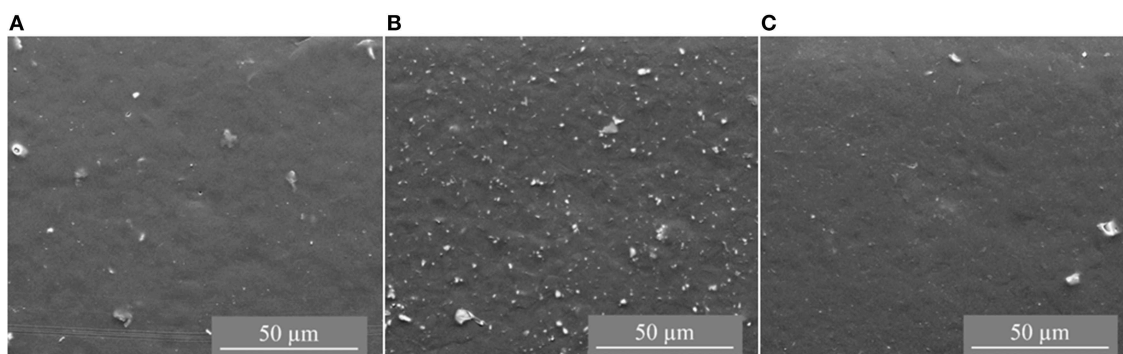


**FIGURE 2** | Top surface SEM images of 8 wt% (A), 16 wt% (B) and 24 wt% (C) of CTF-1@PSF composite MMMs.

cooling to room temperature. The black product was stirred with water for 72 h. Afterwards the product was isolated by filtration and again stirred with 200 mL of 2 mol/L aqueous HCl for 24 h. The resulting black powder was further washed with water, tetrahydrofuran (THF), acetone and dried under vacuum (yield 90 %).

### Preparation of MMMs

The MMMs were prepared with 0, 8, 16, and 24 wt% of CTF-1. The filler loadings were calculated according to the following equation (6) where the filler mass must be divided by the total mass of the composite:

$$\text{Filler loading (wt\%)} = \frac{m_{\text{filler}}}{m_{\text{polymer}} + m_{\text{filler}}} \times 100 \% \quad (6)$$

The PSF polymer (300 mg) was dissolved in chloroform ( $\text{CHCl}_3$ ) and CTF-1 was added to the polymer solution. The obtained dispersion was stirred for 1 week. Afterwards, the casting solution was treated for 30 min in an ultrasonic bath and was stirred for 30 min again. This cycle was repeated three times. Before casting, the dispersion was kept under stirring for 30 more minutes. The dispersion was cast into metal rings placed on a flat glass surface. A paper tissue covered funnel which was placed

over the membrane after casting to prevent the contamination from dust particles as well as to control the evaporation rate. After solvent evaporation, the membrane was removed from the metal ring and was dried in a vacuum oven at  $120^\circ\text{C}$  overnight. The evaporation of  $\text{CHCl}_3$  from the membrane dispersion forms smooth defect/crack free films upon evaporation. The preparation of MMMs with weight percentages higher than 24 was not possible due to instability and brittleness of the resulting membranes.

## RESULTS AND DISCUSSION

### Characterization of MMMs

The synthesized membranes were characterized by scanning electron microscopy (SEM) with the images depicted in **Figures 1–3**. **Figure 1** shows the top side and cross-section of a pure PSF flat membrane cast from  $\text{CHCl}_3$ .

The CTF-1 composite MMMs had black appearance and were more brittle than the pure PSF membrane. **Figures 2, 3** depict top surface (air side) and cross section images of 8, 16, and 24 wt% of CTF-1 composite MMMs, respectively. **Figure 2** shows some, but rather few, of the CTF-1 particles at the top surfaces of the membranes. In case of sedimentation the specifically less dense CTF-1 particles should collect at the upper surface of the  $\text{CH}_2\text{Cl}_2$

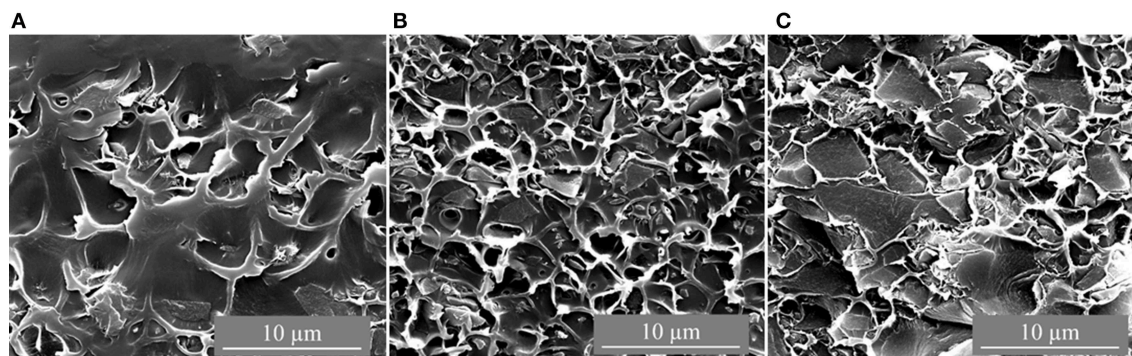


**FIGURE 3** | Cross-section SEM images of 8 wt% (A), 16 wt% (B) and 24 wt% (C) of CTF-1@PSF MMM.

**TABLE 1** | Gas permeabilities ( $O_2$ ,  $N_2$ ,  $CO_2$ ,  $CH_4$ ) and ideal selectivity factors ( $O_2/N_2$ ,  $CO_2/CH_4$ ,  $CO_2/N_2$ ) for the pure PSF and CTF-1@PSF composite membranes.

CTF-1 load (wt%)	P		P		S		
	$O_2$ (Barrer)	$N_2$ (Barrer)	$CO_2$ (Barrer)	$CH_4$ (Barrer)	$O_2/N_2$	$CO_2/N_2$	$CO_2/CH_4$
0	$1.6 \pm 0.0$	$0.3 \pm 0.0$	$7.3 \pm 0.2$	$0.3 \pm 0.0$	$5 \pm 1$	$23 \pm 3$	$21 \pm 3$
8	$2.1 \pm 0.1$	$0.4 \pm 0.0$	$9.2 \pm 0.6$	$0.4 \pm 0.0$	$5 \pm 1$	$23 \pm 3$	$21 \pm 3$
16	$2.2 \pm 0.1$	$0.4 \pm 0.0$	$10.7 \pm 0.6$	$0.5 \pm 0.0$	$5 \pm 1$	$24 \pm 3$	$21 \pm 3$
24	$2.6 \pm 0.2$	$0.5 \pm 0.0$	$12.7 \pm 0.8$	$0.6 \pm 0.0$	$5 \pm 1$	$26 \pm 3$	$22 \pm 3$

From exemplary case studies where we had the same membrane prepared several times and measured each of these membranes also several times we can generally deduce an error of 6% for permeability and 12% for selectivity through error propagation (6% + 6% for each gas permeability).

dispersion, which is obviously not the case. The SEM images of the membrane cross-sections (Figure 3) also indicate uniform dispersion of the CTF-1 material in the polymer matrix and no sedimentation of the CTF-1 particles was visible. The difference of the CTF-1 loading resulted in variation in the thickness of the composite membranes (Table S4). The surface images showed the incorporation of the CTF-1 particles into the polymer matrix which indicate the strong interfacial contact between PSF and CTF-1 material. The visible CTF-1 content is increased with its loading.

## Gas Permeability and Selectivity

In order to examine the gas separation performance of the pure PSF membrane and CTF-1@PSF MMMs, single-gas ( $O_2$ ,  $N_2$ ,  $CO_2$ , and  $CH_4$ ) permeation was carried out at 25°C and 3 bar. The gas permeabilities ( $O_2$ ,  $N_2$ ,  $CO_2$ ,  $CH_4$ ) and ideal selectivity factors ( $O_2/N_2$ ,  $CO_2/CH_4$ ,  $CO_2/N_2$ ) for the pure PSF and CTF-1@PSF composite membranes are provided in Table 1. For dense polymer membranes, gas separation is usually explained by a solution–diffusion mechanism (Pandey and Chauhan, 2001; Tanh Jeazet et al., 2012), which states the permeability of gas molecules through membrane as a product of diffusivity ( $D$ ) and solubility ( $S$ ) (Chung et al., 2007):

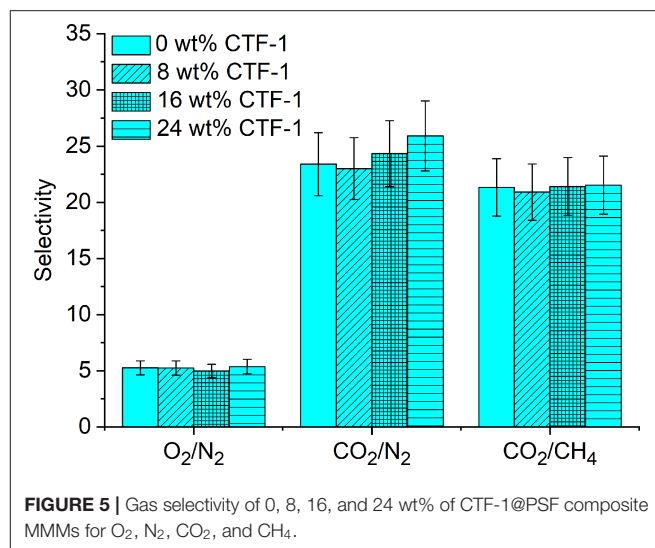
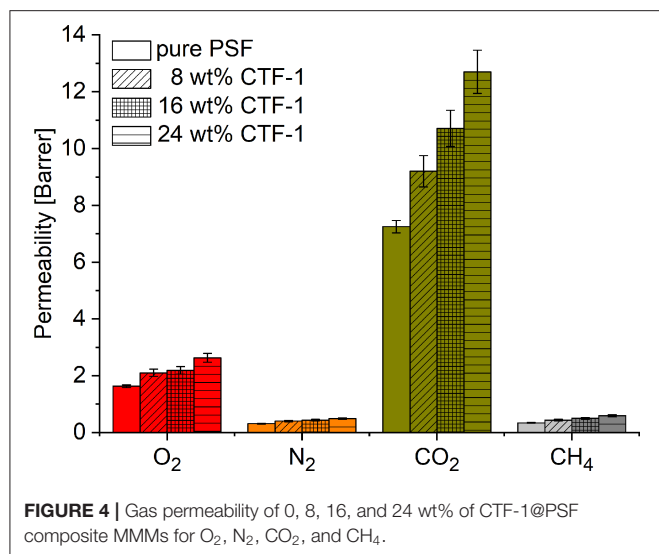
$$P = D \times S \quad (7)$$

Diffusivity is the mobility of individual gas molecules passing through the voids between the polymeric chains of a membrane whereas gas solubility is controlled by the affinity of gas molecules toward the polymer. Addition of fillers to the polymeric membrane may affect both diffusivity and solubility which is

related to physical properties of the fillers like particle size and particle agglomerations, and the polymer/particle interface morphologies, although the trend may not always be the same (Shan et al., 2016).

The permeability for the gases increases in proportion to the amount of CTF-1 present in the MMMs (Figure 4). The highest permeability for all the gases was found for the 24 wt% CTF-1@PSF membrane. The  $O_2$  permeability is increased by 63 % (from 1.6 to 2.6 Barrer),  $N_2$  permeability by 67 % (from 0.3 to 0.5 Barrer),  $CO_2$  permeability by 74 % (from 7.3 to 12.7 Barrer), and  $CH_4$  permeability is increased by 100 % (from 0.3 to 0.6 Barrer).

Figure 5 shows the graphical representation of the ideal selectivity values. There is no significant improvement observed for  $O_2/N_2$  and  $CO_2/CH_4$  selectivity. On the other hand,  $CO_2/N_2$  selectivity was found to be increased from 23 to 26. Selective  $CO_2$  over  $N_2$  adsorption of pure CTF-1 (Figure S7; Section Ideal Adsorbed Solution Theory (IAST) Calculation in the Supplementary Material) was confirmed by application of IAST (Myers and Prausnitz, 1965). The ideal selectivity factor for a binary  $CO_2/N_2$  gas mixture at 1 bar pressure at 293 K is 46 and therefore explains the increase of selectivity with higher filler content in the MMMs. The higher  $CO_2$  permeability as well as  $CO_2/N_2$  separation factors measured for the MMMs can be rationalized by the selective adsorption of  $CO_2$  in the nitrogen rich CTF-1 through dipole–quadrupole interactions (Li et al., 2014). When porous fillers (i.e., CTF-1) are added, the solubility may increase which is due to the higher affinity of  $CO_2$  toward CTF-1, as well as selective diffusivity may increase as the free volume of MMMs increases. The presence of the microporous



CTF with pore diameters mainly distributed at 5, 6, and 12 Å could also exert some preferential sieving of CO<sub>2</sub> (kinetic diameter of 0.33 nm) over N<sub>2</sub> (0.364 nm) or CH<sub>4</sub> (0.38 nm) (Li et al., 2004; Cecopieri-Gómez et al., 2007).

Generally, POPs or COFs (albeit not CTFs) were already used as filler materials in different MMMs for example with the polymers polybenzimidazole (PBI), Matrimid, or polyvinylamine (PVAm). Kang et al. incorporated two 2D COFs NUS-2 and NUS-3 as a filler in a polymer matrix (Ultem and PBI) and the membrane with 20 wt% of NUS-2 loading in PBI exhibited a H<sub>2</sub>/CO<sub>2</sub> selectivity of 31.4 on single gas tests at high pressure which surpassed the 2008 Robeson upper bound limit (Kang et al., 2016). Shan et al. reported a MMM, using Matrimid and an azine linked COF i.e., ACOF-1, where the MMM with 16 wt% of ACOF-1 showed a CO<sub>2</sub> permeability two times higher than the pure Matrimid membrane (Shan et al., 2016). A more than 3-fold elevation in CO<sub>2</sub> permeability compared to the pure PVAm membrane was reported with an imine-based COF (COF-LZU1) as filler (Cao et al., 2016). Fu et al. synthesized a COF/MOF (COF-300/ZIF-8) composite membrane which gives a H<sub>2</sub>/CO<sub>2</sub> selectivity of 13.5 in comparison to the respective COF-300 (6.0) and ZIF-8 (9.1) membranes (Fu et al., 2016). Biswal et al. introduced two hybrid membranes such as TpPa-1@PBI-BuI and TpBD@PBI-BuI (BuI = 5-t-butylisophthalic acid). Almost seven times higher permeabilities for the gases H<sub>2</sub>, N<sub>2</sub>, CO<sub>2</sub>, and CH<sub>4</sub> could be achieved compared to the pure polymer membranes (Biswal et al., 2016). These aforementioned types of POPs have, however, low chemical and thermal stability, which limits the use for MMM based gas separation. Porous CTFs on the other hand, feature high thermal and chemical stability and often show a high CO<sub>2</sub> uptake capacity and good selectivity toward CO<sub>2</sub>/N<sub>2</sub> (Zhao et al., 2013; Hug et al., 2015).

So far, no CTF-based mixed-matrix membranes have been studied for gas permeation, to the best of our knowledge. A direct comparison can be made to a pure CTF membrane, named TFM-1 derived from 4,4'-biphenyldicarbonitrile (DCBP). The

single gas CO<sub>2</sub>/N<sub>2</sub> selectivity value of 26 for the 24 wt% CTF-1 membrane is comparable to CO<sub>2</sub>/N<sub>2</sub> selectivity of this pure TFM-1 membrane (29 ± 2) (Zhu et al., 2012). Further, we can compare our CTF-1@PSF MMMs only to related porous organic polymer MMMs. From an N-rich Schiff based porous organic framework (SNW-1) which was constructed from melamine and di-aldehydes the derived best PSF-MMMs yielded higher CO<sub>2</sub> and N<sub>2</sub> gas permeabilities than CTF-1@PSF but a similar CO<sub>2</sub>/N<sub>2</sub> selectivity of 29 in single gas measurements (Gao et al., 2014). The CO<sub>2</sub> permeability of 12.7 Barrer and the selectivity of 26 in the 24 wt% CTF-1@PSF MMM is similar or even slightly better to the performance of the azobenzene-based nanoporous polymer, called Azo-COP-2, in a PSF matrix with 14.8 Barrer and a CO<sub>2</sub>/N<sub>2</sub> selectivity of 23 (Li et al., 2019).

We have also performed mixed gas separation measurements for 400 mg PSF membranes (Table S5) for 8 and 16 wt% CTF-1@PSF MMMs. The selectivities of 8 wt% and 16 wt% of CTF-1 loading MMMs for an equimolar (50/50) gas mixture of CO<sub>2</sub> and CH<sub>4</sub> were found to be 40 and 42 which is higher than the single gas selectivity. Compared to single gas permeation tests, mixed gas permeation tests give higher selectivity due to the competitive adsorption and diffusion of the binary gas components in the membrane. Due to the smaller molecular size and high affinity of the CO<sub>2</sub> molecule to the basic triazine unit of CTF-1, CO<sub>2</sub> favorably adsorbed to the CTF-1 loaded MMMs, which reduces the diffusion of CH<sub>4</sub> in the membranes due to pore blocking by adsorbed CO<sub>2</sub> (Kang et al., 2016).

## Maxwell Model

A way to predict the permeability of MMMs is the application of the Maxwell model. In its original form it can be used for low filler contents ( $\phi_d$  up to 0.2), to exclude interactions among the filler particles (Bouma et al., 1997; Kanehashi et al., 2015). The Maxwell equation can be expressed by Equation (8):

$$P_{eff} = P_c \times \frac{P_d + 2P_c - 2\phi_d \times (P_c - P_d)}{P_d + 2P_c + \phi_d \times (P_c - P_d)} \quad (8)$$

$P_d$  is given as the filler permeability and  $P_c$  is the permeability of the pure polymer membrane.  $\phi_d$  is the volume fraction of the filler phase according to Equation (9).

$$\phi_d = \frac{w_d / \rho_d}{\frac{w_c}{\rho_c} + \frac{w_d}{\rho_d}} \quad (9)$$

A “reduced permeation polarizability”  $\beta$  can be defined as given in Equation (10) (Basu et al., 2010),

$$\beta = \frac{P_d - P_c}{P_d + 2P_c} \quad (10)$$

and consequently Equation (8) can be simplified to Equation (11):

$$P_{eff} = P_c \times \frac{1 + 2\beta \times \phi_d}{1 - \beta \times \phi_d} \quad (11)$$

The value of  $\beta$  describes the difference in permeability between the continuous or polymer phase (with  $P_c$ ) and the dispersed or filler phase (with  $P_d$ ). There are three limiting cases which can be considered: The filler is much more permeable than the polymer, that is  $P_d \gg P_c$  and  $\beta \approx 1$ ; both filler and polymer are equally permeable, that is  $P_d = P_c$  and  $\beta = 0$  and the filler is non-permeable or  $P_d \ll P_c$  and  $\beta \approx -0.5$  (Basu et al., 2010). In case of CTF-1 being regarded as a highly-permeable filler material ( $P_d \gg P_c$ ), the following equation (12) is used:

$$\frac{P_{eff}}{P_c} = \frac{1 + 2\phi_d}{1 - \phi_d} \quad (12)$$

The plot  $P_{eff}/P_c$  vs.  $\phi_d$  is presented in **Figure 6**. The comparison with the theoretical Maxwell plot shows an agreement only in the range of very low filler contents. With a higher volume fraction of

the filler, the theoretical Maxwell model predicts a higher increase in permeability. The Maxwell model describes an ideal case, which is also based on the assumption of an ideal distribution of the filler particles and the spherical shape of the filler particles (Bouma et al., 1997). The deviation from the model could be explained by the non-spherical shape of the CTF-1 particles. Another reason could be the penetration of PSF polymer chains into the pores of CTF-1 and thus a loss of free volume of the filler (Li et al., 2005).

If the pores in CTF-1 would be fully blocked and the filler thereby becomes nearly non-permeable we have the limiting case of  $P_d \ll P_c$  and  $\beta \approx -0.5$  with equation (13), with the plot of  $P_{eff}/P_c$  vs.  $\phi_d$  also included in **Figure 6**:

$$\frac{P_{eff}}{P_c} = \frac{1 - \phi_d}{1 + 0.5\phi_d} \quad (13)$$

From **Figure 6** it is evident that the measured permeability lies between the limiting case with  $P_d \gg P_c$  and the case where both filler and polymer are equally permeable, that is  $P_d = P_c$  with  $P_{eff}/P_c = 1$ . In order to therefore approximate the experimental permeability, we can assume  $P_d = 6P_c$  with  $\beta = 0.625$  to give Equation (14):

$$\frac{P_{eff}}{P_c} = \frac{1 + 1.25\phi_d}{1 - 0.625\phi_d} \quad (14)$$

The plot of Equation (14) is depicted in **Figure 6** and the experimental values show good agreement with the model.

An overview of other models for the case  $P_d \gg P_c$ , including Bruggeman (1935), Higuchi (Higuchi and Higuchi, 1960; Shen and Lua, 2013), and Böttcher-Landauer (Hashin and Shtrikman, 1962) for  $P_{eff}/P_c$  vs. filler fraction is given in **Figure S9** (Section Other Permeability Models for 300 mg Membranes in the **Supplementary Material**). It is evident that the other models overestimate the permeability even more strongly than the Maxwell model for  $P_d \gg P_c$ .

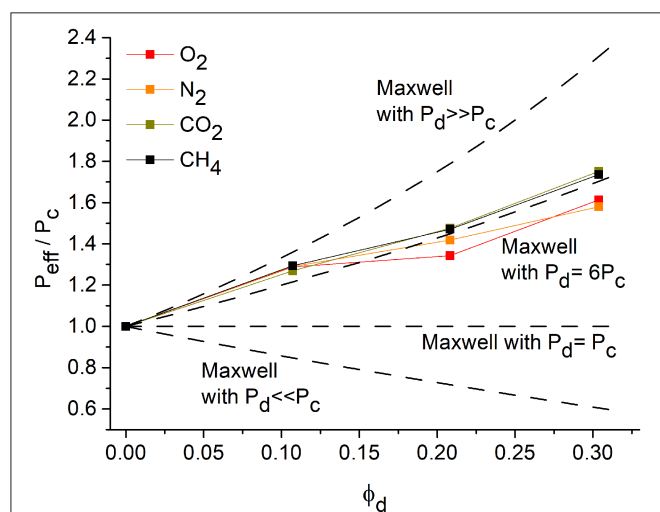


**FIGURE 6** |  $P_{eff}/P_c$  vs.  $\phi_d$ . Measured permeabilities for the pure polymer and the polymer with 8, 16, and 24 wt% of the filler in comparison to the Maxwell model with different relations between  $P_{eff}$  and  $P_c$  (dashed lines).

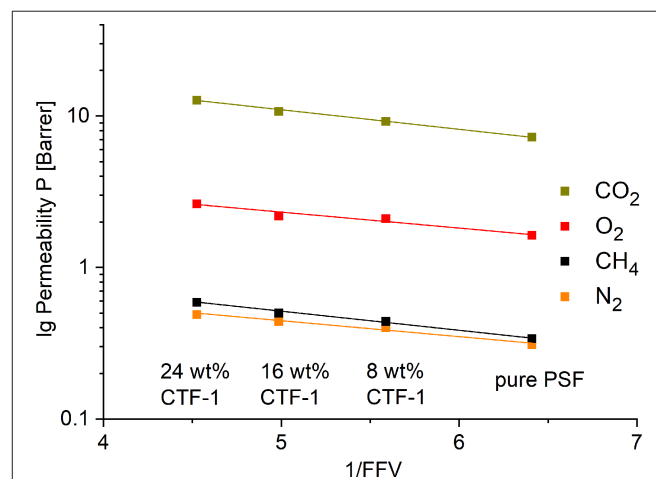


**FIGURE 7** | Logarithmic plot of the experimental  $O_2$ ,  $N_2$ ,  $CO_2$ , and  $CH_4$  permeabilities vs. the inverse (total) FFV of the pure polymer and the polymer with 8, 16, and 24 wt% of the filler.

## Fractional Free Volume (FFV)

The FFV of the filler was calculated by multiplication of the density ( $\rho_d$  in  $\text{g}/\text{cm}^3$ ) and the pore volume ( $\text{cm}^3/\text{g}$ ) (Thran et al., 1999). He-pycnometry combined with BET-sorption measurement was used to determine the density ( $\rho_d$ ) of CTF-1 ( $\rho_d = 0.89 \text{ g}/\text{cm}^3$ , dispersed phase) and the pore volume of  $0.42 \text{ cm}^3/\text{g}$  was given by BET-sorption analysis. The density of PSF ( $\rho_c = 1.23 \text{ g}/\text{cm}^3$ , continuous phase) as well as the  $\text{FFV}_{\text{polymer}}$  (0.156) is used according to the literature (Thran et al., 1999; Anaya et al., 2014). In order to calculate the (total) FFV of the MMM both the FFV of the polymer and of the filler are multiplied by their respective volume fractions,  $\phi_c$  and  $\phi_d$ , and summed up according to Equation (15). The volume fraction of the polymer  $\phi_c$  was determined in analogy to Equation (9).

$$(\text{total})\text{FFV} = \text{FFV}_{\text{polymer}} \times \phi_c + \text{FFV}_{\text{filler}} \times \phi_d \quad (15)$$

Figure 7 presents the logarithm of the measured gas permeabilities ( $\lg P$ ) for  $\text{O}_2$ ,  $\text{N}_2$ ,  $\text{CO}_2$ , and  $\text{CH}_4$  as a function of the inverse FFV for pure PSF, 8, 16, and 24 wt% of CTF-1. The FFV for 8 wt% of the filler is 0.18, loadings of 16 and 24 wt% show values of 0.20 and 0.22. Independent from gas all plots show a linear correlation.

## CONCLUSION

In summary, we have successfully synthesized for the first time mixed matrix membranes containing thermally and chemically stable CTF-1 and PSF. Overall six MMMs have been casted in this study by using PSF with 8, 16, and 24 wt% CTF-1. The SEM images of the membrane cross-sections show uniform dispersion of the CTF-1 material in the polymer matrix, whereas the surface images of the MMMs indicate the strong interfacial contact between PSF and CTF-1 material. The fabricated membranes exhibit higher  $\text{CO}_2$  permeabilities (12.7 Barrer for 24 wt% of CTF-1 loading) than the pure PSF membrane (7.3 Barrer). For other gases there are no significant improvements in the permeability. The MMMs show higher  $\text{CO}_2/\text{N}_2$  selectivity (26 for 24 wt% of CTF-1 loading) compared to pure PSF membrane (23), the selectivity increases with increasing of CTF loading. The results for higher filler contents differ from the Maxwell model

for porous fillers, but a constant increase of permeability can be observed for the gases  $\text{CO}_2$  and  $\text{CH}_4$  and a modified Maxwell model was successfully applied. The increased gas permeability follows linearly the inverse of the total free fractional volume, which indicates that both free fractional volume of the polymer and the filler contribute to the permeability.

## DATA AVAILABILITY STATEMENT

All datasets generated for this study are included in the article/**Supplementary Material**.

## AUTHOR CONTRIBUTIONS

SD synthesized membranes and wrote half of the manuscript. SB wrote half of manuscript and applied permeability models, FFV, and drew the graphics. SS carried out mixed gas measurements. AN participated in calculations for Maxwell model and FFV. AB provided CTF-1 and related analytical information. JC was involved in mixed gas measurements and interpretation. CJ proofread and refined the manuscript.

## FUNDING

Open access publication fees were covered by Heinrich-Heine-University.

## ACKNOWLEDGMENTS

Financial support from the Spanish MINECO and FEDER (MAT2016-77290-R), the Aragón Government (T43-17R), and the ESF was gratefully acknowledged by JC. The work of CJ was supported by the Federal German Ministry of Education and Research (BMBF) under grant Optimat 03SF0492C.

## SUPPLEMENTARY MATERIAL

The Supplementary Material for this article can be found online at: <https://www.frontiersin.org/articles/10.3389/fchem.2019.00693/full#supplementary-material>

## REFERENCES

- Anaya, S., Serrano, B., Herrero, B., Cervera, A., and Baselga, J. (2014).  $\gamma$ -alumina modification with long chain carboxylic acid surface nanocrystals for biocompatible polysulfone nanocomposites. *ACS Appl. Mater. Interfaces* 6, 14460–14468. doi: 10.1021/am503744z
- Baker, R. W. (2002). Future directions of membrane gas separation technology. *Ind. Eng. Chem. Res.* 41, 1393–1411. doi: 10.1021/ie0108088
- Bastani, D., Esmaili, N., and Asadollahi, M. (2013). Polymeric mixed matrix membranes containing zeolites as a filler for gas separation applications: a review. *J. Ind. Eng. Chem.* 19, 375–393. doi: 10.1016/j.jiec.2012.09.019
- Basu, S., Cano-Odena, A., and Vankelecom, I. F. J. (2010). Asymmetric Matrimid®/[Cu<sub>3</sub>(BTC)<sub>2</sub>] mixed-matrix membranes for gas separations. *J. Membr. Sci.* 362, 478–487. doi: 10.1016/j.memsci.2010.07.005
- Bhunia, A., Vasylyeva, V., and Janiak, C. (2013). From a supramolecular tetranitrile to a porous covalent triazine-based framework with high gas uptake capacities. *Chem. Commun.* 49, 3961–3963. doi: 10.1039/c3cc41382a
- Biswal, B. P., Chaudhari, H. D., Banerjee, R., and Kharul, U. K. (2016). Chemically stable covalent organic framework (COF)-polybenzimidazole hybrid membranes: enhanced gas separation through pore modulation. *Chem. Eur. J.* 22, 4695–4699. doi: 10.1002/chem.201504836
- Bouma, R. H. B., Checchetti, A., Chidichimo, G., and Drioli, E. (1997). Permeation through a heterogeneous membrane: the effect of the dispersed phase. *J. Membr. Sci.* 128, 141–149. doi: 10.1016/S0376-7388(96)00303-1
- Bruggeman, D. A. G. (1935). Berechnung verschiedener physikalischer Konstanten von heterogenen Substanzen. I. Dielektrizitätskonstanten und Leitfähigkeiten der Mischkörper aus isotropen Substanzen. *Ann. Phys.* 24, 636–679. doi: 10.1002/andp.19354160705

- Buonomenna, M. G., Yave, W., and Golemme, G. (2012). Some approaches for high performance polymer based membranes for gas separation: block copolymers, carbon molecular sieves and mixed matrix membranes, *RSC Adv.* 2, 10745–10773. doi: 10.1039/c2ra20748f
- Cao, X., Qiao, Z., Wang, Z., Zhao, S., Li, P., Wang, J., et al. (2016). Enhanced performance of mixed matrix membrane by incorporating a highly compatible covalent organic framework into poly(vinylamine) for hydrogen purification. *Int. J. Hydrogen Energy* 41, 9167–9174. doi: 10.1016/j.ijhydene.2016.01.137
- Cecopieri-Gómez, M. L., Palacios-Alquisira, J., and Domínguez, J. M. (2007). On the limits of gas separation in CO<sub>2</sub>/CH<sub>4</sub>, N<sub>2</sub>/CH<sub>4</sub> and CO<sub>2</sub>/N<sub>2</sub> binary mixtures using polyimide membranes. *J. Membr. Sci.* 293, 53–65. doi: 10.1016/j.memsci.2007.01.034
- Chung, T.-S., Jiang, L. Y., Li, Y., and Kulprathipanja, S. (2007). Mixed matrix membranes (MMMs) comprising organic polymers with dispersed inorganic fillers for gas separation. *Prog. Polym. Sci.* 32, 483–507. doi: 10.1016/j.progpolymsci.2007.01.008
- Dechnik, J., Gascon, J., Doonan, C. J., Janiak, C., and Sumbly, C. J. (2017). Mixed-matrix membranes. *Angew. Chem. Int. Ed.* 56, 9292–9310. doi: 10.1002/anie.201701109
- Dechnik, J., Mühlbach, F., Dietrich, D., Wehner, T., Gutmann, M., Luhmann, T., et al. (2016). Luminescent metal–organic framework mixed–matrix membranes from lanthanide metal–organic frameworks in polysulfone and matrimid. *Eur. J. Inorg. Chem.* 4408–4415. doi: 10.1002/ejic.201600235
- Dey, S., Bhunia, A., Boldog, I., and Janiak, C. (2017). A mixed-linker approach towards improving covalent triazine-based frameworks for CO<sub>2</sub> capture and separation. *Micropor. Mesopor. Mater.* 241, 303–315. doi: 10.1016/j.micromeso.2016.11.033
- Dong, G., Li, H., and Chen, V. (2013). Challenges and opportunities for mixed-matrix membranes for gas separation. *J. Mater. Chem. A* 1, 4610–4630. doi: 10.1039/c3ta00927k
- Fu, J., Das, S., Xing, G., Ben, T., Valtchev, V., and Qiu, S. (2016). Fabrication of COF-MOF composite membranes and their highly selective separation of H<sub>2</sub>/CO<sub>2</sub>. *J. Am. Chem. Soc.* 138, 7673–7680. doi: 10.1021/jacs.6b03348
- Gao, X., Zou, X., Ma, H., Meng, S., and Zhu, G. (2014). Highly selective and permeable porous organic framework membrane for CO<sub>2</sub> capture. *Adv. Mater.* 26, 3644–3648. doi: 10.1002/adma.201400020
- Hashin, Z., and Shtrikman, A. (1962). Variational approach to the theory of the effective magnetic permeability of multiphase materials. *J. Appl. Phys.* 33, 3125–3131. doi: 10.1063/1.1728579
- Higuchi, W. I., and Higuchi, T. (1960). Theoretical analysis of diffusional movement through heterogeneous barriers. *J. Am. Pharm. Assoc. Sci.* 49, 598–606. doi: 10.1002/jps.3030490910
- Hug, S., Stegbauer, L., Oh, H., Hirscher, M., and Lotsch, B. V. (2015). Nitrogen-rich covalent triazine frameworks as high-performance platforms for selective carbon capture and storage. *Chem. Mater.* 27, 8001–8010. doi: 10.1021/acs.chemmater.5b03330
- Kanehashi, S., Chen, G. Q., Scholes, C. A., Ozcelik, B., Hua, C., Ciddor, L., et al. (2015). Enhancing gas permeability in mixed matrix membranes through tuning the nanoparticle properties. *J. Membr. Sci.* 482, 49–55. doi: 10.1016/j.memsci.2015.01.046
- Kang, Z., Peng, Y., Qian, Y., Yuan, D., Addicoat, M. A., Heine, T., et al. (2016). Mixed matrix membranes (MMMs) comprising exfoliated 2D covalent organic frameworks (COFs) for efficient CO<sub>2</sub> separation. *Chem. Mater.* 28, 1277–1285. doi: 10.1021/acs.chemmater.5b02902
- Koros, W. J., and Fleming, G. K. (1993). Membrane-based gas separation. *J. Membr. Sci.* 83, 1–80. doi: 10.1016/0376-7388(93)80013-N
- Kuhn, P., Antonietti, M., and Thomas, A. (2008). Porous, covalent triazine-based frameworks prepared by ionothermal synthesis. *Angew. Chem. Int. Ed.* 47, 3450–3453. doi: 10.1002/anie.200705710
- Li, S., Falconer, J. L., and Noble, R. D. (2004). SAPO-34 membranes for CO<sub>2</sub>/CH<sub>4</sub> separation. *J. Membr. Sci.* 241, 121–135. doi: 10.1016/j.memsci.2004.04.027
- Li, S., Prasetya, N., and Ladewig, B. P. (2019). Investigation of Azo-COP-2 as a photoresponsive low-energy CO<sub>2</sub> adsorbent and porous filler in mixed matrix membranes for CO<sub>2</sub>/N<sub>2</sub> separation. *Ind. Eng. Chem. Res.* 58, 9959–9969. doi: 10.1021/acs.iecr.9b00762
- Li, Y., Chung, T.-S., Cao, C., and Kulprathipanja, S. (2005). The effects of polymer chain rigidification, zeolite pore size and pore blockage on polyethersulfone (PES)-zeolite A mixed matrix membranes. *J. Membr. Sci.* 260, 45–55. doi: 10.1016/j.memsci.2005.03.019
- Li, Z., Feng, X., Zou, Y., Zhang, Y., Xia, H., Liu, X., et al. (2014). A 2D azine-linked covalent organic framework for gas storage applications. *Chem. Commun.* 50, 13825–13828. doi: 10.1039/C4CC05665E
- Myers, A. L., and Prausnitz, J. M. (1965). Thermodynamics of mixed-gas adsorption. *AICHE J.* 11, 121–127. doi: 10.1002/aic.690110125
- Pandey, P., and Chauhan, R. S. (2001). Membranes for gas separation. *Prog. Polym. Sci.* 26, 853–893. doi: 10.1016/S0079-6700(01)00009-0
- Shan, M., Seoane, B., Rozhko, E., Dikhtiarenko, A., Clet, G., Kapteijn, F., et al. (2016). Azine-linked covalent organic framework (COF)-based mixed-matrix membranes for CO<sub>2</sub>/CH<sub>4</sub> separation. *Chem. Eur. J.* 22, 14467–14470. doi: 10.1002/chem.201602999
- Shen, Y., and Lua, A. I. (2013). Theoretical and experimental studies on the gas transport properties of mixed matrix membranes based on polyvinylidene fluoride. *AICHE J.* 59, 4715–4726. doi: 10.1002/aic.14186
- Shimekit, B., Mukhtar, H., and Murugesan, T. (2011). Prediction of the relative permeability of gases in mixed matrix membranes. *J. Membr. Sci.* 373, 152–159. doi: 10.1016/j.memsci.2011.02.038
- Strathmann, H. (2001). Membrane separation processes: current relevance and future opportunities. *AICHE J.* 47, 1077–1087. doi: 10.1002/aic.690470514
- Tang, Y. P., Wang, H., and Chung, T. S. (2015). Towards high water permeability in triazine-framework-based microporous membranes for dehydration of ethanol. *ChemSusChem* 8, 138–147. doi: 10.1002/cssc.201402816
- Tanh Jeazet, H. B., Sorribas, S., Román-Marín, J. M., Zornoza, B., Téllez, C., and Coronas, J. (2016). Increased selectivity in CO<sub>2</sub>/CH<sub>4</sub> separation with mixed-matrix membranes of polysulfone and mixed-MOFs MIL-101(Cr) and ZIF-8. *Eur. J. Inorg. Chem.* 27, 4363–4367. doi: 10.1002/ejic.201600190
- Tanh Jeazet, H. B., Staudt, C., and Janiak, C. (2012). Metal–organic frameworks in mixed-matrix membranes for gas separation. *Dalton Trans.* 41, 14003–14027. doi: 10.1039/c2dt31550e
- Thran, S., Kroll, G., and Faubel, F. (1999). Correlation between fractional free volume and diffusivity of gas molecules in glassy polymers. *J. Polym. Sci. B* 37, 3344–3358. doi: 10.1002/(SICI)1099-0488(19991201)37:23<3344::AID-POLB10>3.0.CO;2-A
- Ying, Y., Liu, D., Ma, J., Tong, M., Zhang, W., Huang, H., et al. (2016). A GO-assisted method for the preparation of ultrathin covalent organic framework membranes for gas separation. *J. Mater. Chem. A* 4, 13444–13449. doi: 10.1039/C6TA04579K
- Zhang, Y., Musselman, I. H., Ferraris, J. P., and Balkus, J. R., K. J. (2008). Gas permeability properties of Matrimid membranes containing the metal-organic framework Cu-BPY-HFS. *J. Membr. Sci.* 313, 170–181. doi: 10.1016/j.memsci.2008.01.005
- Zhao, Y. F., Yao, K. X., Teng, B. Y., Zhang, T., and Han, Y. (2013). A perfluorinated covalent triazine-based framework for highly selective and water-tolerant CO<sub>2</sub> capture. *Energy Environ. Sci.* 6, 3684–3692. doi: 10.1039/c3ee42548g
- Zhu, X., Tian, C., Mahurin, S. M., Chai, S.-H., Wang, C., Brown, S., et al. (2012). A Superacid-catalyzed synthesis of porous membranes based on triazine frameworks for CO<sub>2</sub> separation. *J. Am. Chem. Soc.* 134, 10478–10484. doi: 10.1021/ja304879c

**Conflict of Interest:** The authors declare that the research was conducted in the absence of any commercial or financial relationships that could be construed as a potential conflict of interest.

Copyright © 2019 Dey, Bügel, Sorribas, Nuhnen, Bhunia, Coronas and Janiak. This is an open-access article distributed under the terms of the Creative Commons Attribution License (CC BY). The use, distribution or reproduction in other forums is permitted, provided the original author(s) and the copyright owner(s) are credited and that the original publication in this journal is cited, in accordance with accepted academic practice. No use, distribution or reproduction is permitted which does not comply with these terms.